# ATOMISTIC STUDIES OF <101] SCREW DISLOCATION CORE STRUCTURES AND GLIDE IN $\gamma$-TiAl

Ivaylo Hristov Katzarov, Anthony T Paxton


# ATOMISTIC STUDIES OF 〈101] SCREW DISLOCATION CORE STRUCTURES AND GLIDE IN γ-TiAl

| | |
|---|---|
| Journal: | *Philosophical Magazine & Philosophical Magazine Letters* |
| Manuscript ID: | TPHM-08-Nov-0398.R2 |
| Journal Selection: | Philosophical Magazine |
| Date Submitted by the Author: | 21-Apr-2009 |
| Complete List of Authors: | Katzarov, Ivaylo; Queen's University Belfast, School of Mathematics and Physics<br>Paxton, Anthony; Queen's University Belfast, School of Mathematics and Physics |
| Keywords: | atomistic simulation, dislocations, titanium aluminides |
| Keywords (user supplied): | atomistic simulation, dislocations, titanium aluminides |
| | |

# ATOMISTIC STUDIES OF $\langle 101]$ SCREW DISLOCATION CORE STRUCTURES AND GLIDE IN γ-TiAl

I. H. KATZAROV and A. T. PAXTON

*Atomistic Simulation Centre, School of Mathematics and Physics, Queens University Belfast, Belfast BT7 1NN, Northern Ireland, U.K.*



## ABSTRACT

This paper focuses on the core structure of $\langle 101]$ superdislocations in $L1_0$ TiAl with the purpose of clarifying their dissociation abilities and the mechanisms by which these may become sessile by self-locking. A detailed knowledge of the fine structure of dislocations is essential in analysing the origin of the various deformation features. Atomistic simulation of the core structure and glide of the screw $\langle 101]$ superdislocation has been made using a bond order potential for γ-TiAl. We have examined the core structure of the screw $\langle 101]$ superdislocation starting with initial unrelaxed configurations corresponding to various dislocation dissociations, discussed in the literature. The superdislocation was found to possess in the screw orientation either planar (glissile) or non-planar (sessile) core structures. We studied the response of our core configurations to externally applied shear stress. We considered some implications of the dissociated configurations and their response to externally applied stress on dislocation dynamics, including the issue of dislocation decomposition, the mechanism of locking and the orientation dependence of the dislocation substructure observed in single-phase γ-TiAl. We find an unexpectedly rich and complex set of candidate core structures both planar and non-planar, whose cores may transform under applied stress with consequent violation of Schmid's law.

## 1. INTRODUCTION

Physical and mechanical properties, such as low density, exceptionally high strength, hardness, creep and corrosion resistance at high temperatures, make γ-based titanium aluminide alloys attractive candidates for high temperature applications in aerospace and automotive industries [1, 2]. Only the γ-TiAl (tetragonal $L1_0$) and $\alpha_2$ $Ti_3Al$ (hexagonal DO19) phases have mechanical properties that are suitable for industrial applications. In spite of promising high temperature properties, the $\alpha_2$ and γ single phase components are both quite brittle and thereby have not attracted much industrial interest. Acceptable combinations of strength, ductility and toughness can be achieved by special heat treatments leading to the formation of a two-phase lamellar microstructure consisting of layers of $\alpha_2$-$Ti_3Al$ and γ-TiAl. It is widely accepted that the γ -phase carries

the vast majority of deformation in two-phase alloys, but a detailed understanding of the mechanical behavior of single-phase γ-TiAl has not been forthcoming. The main deformation modes in γ-TiAl are slip and twinning, both of which operate on one of the close-packed $\{111\}$ planes [3]. Slip occurs via two types of dislocations: ordinary dislocations with Burgers vector $\frac{1}{2}\langle 110]$, and $\langle 101]$ superdislocations. The observed twinning is along the $\langle 112]$ direction. In single γ crystals, superdislocations dominate at low temperatures and the glide of ordinary dislocations and twinning become significant only at high temperatures [3, 4]. We use Burgers vector notations for tetragonal crystals [5].

Understanding of these deformation properties can not be achieved in the framework of the standard elastic theory of dislocations since core phenomena are likely to play an important role. The only plausible way of studying such phenomena is by means of atomistic simulations. A number of atomistic studies of the core structure and properties of dislocations in single-phase $L1_0$-TiAl have been made by previous authors [6–9]. In most of these studies, pair functionals were used to describe the atomic interactions in the material. While calculations employing central-force schemes revealed a number of general features of dislocations that can be expected in the $L1_0$ structure, they do not capture effects arising from the covalent and directional bonding characteristic of TiAl. The core structure and friction barrier of the ordinary $\frac{1}{2}\langle 110]$ dislocation was also studied using ab initio density-functional theory (DFT) [10]. First principles methods based on DFT provide a reliable description of the interatomic forces, but are limited by feasible block sizes that contain not more than a couple of hundred atoms and usually require use of periodic boundary conditions that are not well suited for dislocation studies.

In order to describe processes of such complexity one has to cross the bridge between the electronic-structure calculations and atomistic simulations by coarse-graining the electronic degrees of freedom into many-body interatomic potentials. Pettifor's bond order potential (BOP) [11, 12] represents a numerically efficient scheme that works within the orthogonal tight binding approximation with environment dependent matrix elements. The multi-atom character of the forces, is thereby captured in a physical way that goes beyond the standard pair functionals (Finnis–Sinclair, EAM). In the framework of BOP, the energy of a system of atoms is divided into three parts. The bond energy, $E_{bond}$ , arises from the formation of the valence band, including terms dependent on bond angles. The neglect of overlap in the orthogonal tight-binding model is corrected by a repulsive environmental energy term, $E_{env}$ , which accounts for the positive pressure from orthogonality constraints between the valence sp states and the atomic core [13]. An additional pairwise repulsive energy, $E_{pair}$ , describes valence-valence overlap, nuclear repulsion and exchange-correlation corrections to the total energy. The environmental repulsive energy is fitted to the Cauchy pressure, which would be constrained to be positive in the absence of this term [14]. $E_{pair}$ is fitted to the remaining elastic constants, the lattice constants and the cohesive energy [15]. Apart from their genuine quantum-mechanical origin, BOPs have two additional important advantages. First, the evaluation of the energy scales linearly in computational time with

the number of atoms, and, second, the real-space formalism avoids the need of imposing full periodic boundary conditions common to k-space methods. Both of these features are crucial for studies of dislocations since such simulations often require a large number of atoms and complex geometries.

Recently, a BOP for γ-TiAl was constructed and extensively tested against accurate first-principles methods in order to assess the potentials reliability and applicability [15, 16]. For dislocation studies the most important are the energies of stacking-fault like defects, whose values calculated by BOP agree well with those found by DFT based calculations [10, 17, 18]. Atomistic simulations of the core structure and glide of the ordinary screw $\frac{1}{2}\langle 110]$ dislocation and the screw $\langle 101]$ superdislocation in single-phase $L1_0$-TiAl have been performed using the BOP [19], which has also been used for atomistic simulations of the core structure and glide of ordinary $\frac{1}{2}\langle 110]$ screw dislocations in two $L1_0$-TiAl lamellae forming a twin γ/γ-interface [20]. These calculations show, in agreement with the ab initio study [10], that $\frac{1}{2}\langle 110]$ ordinary dislocations in the γ phase material have non-planar core structure, spread in the $(111)$ and $(1\bar{1}1)$ planes. The core structure is sessile due to its non-planarity. The $\langle 101]$ superdislocation has two alternative core configurations. The first one is planar and corresponds to splitting into three partials with a superlattice intrinsic stacking fault (SISF) and complex stacking fault (CSF) on $\{111\}$ planes. The second is non-planar and corresponds to the splitting into three partials with ribbons of SISF on $(111)$ and $(1\bar{1}1)$ planes. The former core structure is glissile and moves at relatively low applied stresses. The latter is sessile but is favored when the energy of the SISF is below a critical value. In spite of the overwhelming role of the $\langle 101]\{111\}$ slip system, the properties of $\langle 101]$ dislocations, including the issue of their dissociation abilities, remain relatively poorly studied atomistically.

Atomistic simulations of dislocations have revealed that the size and geometry of the simulation cells in these calculations have to be considered carefully. For long straight dislocations, we may use a periodicity of one or two lattice vectors along the dislocation line, but should avoid using periodic boundary conditions in the other two directions since the dislocation strain field is very long ranged. The cells used in these simulations, as in most real space calculations, are divided into two regions of relaxing and non relaxing atoms, the latter bounded by a free surface sufficiently far from the core to avoid image stresses. Great care must be taken in defining the dimension of the "active" region; it must be large enough, such that the atoms in the exterior region do not impede the relaxation of the interior region. The size of the relaxed region is critical for the determination of the correct core structures, especially in the case of broadly dissociated dislocations such as the $\langle 101]$ screw superdislocation. Even larger active regions are necessary for studying the glide of $\langle 101]$ screw dislocations, because the dislocation can glide a considerable distance before its core structure transforms to a new one under the effect of externally applied shear stress.

The simulations of the screw orientation of the superdislocation, which is the most interesting since it gives rise to possible non-planar dissociations and core spreading, must be run with very large "active" regions. Since the calculations using BOPs are computationally much more demanding than those with standard empirical potentials such simulations are still very challenging. At present all simulations using BOPs are carried out with a version of the OXON program [21] incorporated into Penn–BOP codes created at the University of Pennsylvania, which is a single processor Fortran 77 program. Parallel computation, in which a large number of processors are employed simultaneously on a single problem, offers dramatic possibilities for performing large-scale and long-time atomistic simulations. The BOP scheme is naturally parallelizable since the evaluation of moments and recursion coefficients, which are needed for the calculation of the total energy, may be performed independently for each atomic site. The parallelization of the BOP code is very important to bring realistic and reliable simulations to problems in complex engineering materials with non trivial bonding. We have developed and tested on large parallel machines a parallel version of the OXON-Penn-BOP code. Parallelization of the OXON-Penn-BOP code greatly improves the complexity of defects that can be studied using these state-of-the-art potentials. For instance the cores $P_1$ and $P_2$, described bellow, can only be distinguished after application of a glide stress and in a large simulation cell. Hence the parallel version of the OXON-Penn-BOP code is essential in accessing this distinction.

This paper focuses on the core structure of $\langle 101]$ superdislocations with the purpose of clarifying their dissociation abilities and the mechanisms by which these may become self-locking through core transformations. A detailed knowledge of the fine structure of dislocations is essential in analysing the origin of the various deformation features. In this paper, we present results of atomistic simulations of the core structure and glide of the screw $\langle 101]$ superdislocation. Calculations using BOP for γ-TiAl and cells with large “active” regions were made with the parallel version of the OXON-Penn-BOP code. We examined the core structure of the screw $\langle 101]$ superdislocation starting with initial unrelaxed configurations corresponding to various dislocation dissociations, discussed in the literature. The starting configurations included twofold and threefold splittings into partials on the $\{111\}$ plane, which involve three stacking-fault like defects, the anti-phase boundary (APB), SISF and CSF. Long-time atomistic molecular-static simulations allowed us to study the effect of applied shear stress on the glide and core structure of the superdislocation, at stresses much higher that the stress at which the dislocation starts to move.

## 2. SIMULATION METHODOLOGY AND RESULTS

### 2.1 Static core structure

Atomistic modeling of the $\langle 101]$ superdislocation in screw orientation was performed as follows. The $L1_0$ TiAl crystal was constructed of four successive $(10\bar{1})$ planes forming one period in the $[10\bar{1}]$ direction, along which periodic boundary

conditions were applied. We set the x, y, and z axis of the simulation cell parallel to the $[1\bar{2}1]$, $[111]$ and $[10\bar{1}]$ directions, respectively. A simulation block consisting of 3456 active and 1344 inert atoms was used in the calculations. The dislocations were introduced into the simulation cell after initial relaxation by displacing all atoms in both regions from their perfect lattice positions according to the corresponding anisotropic elastic displacement field [22]. A molecular statics method of minimizing the energy of the system was employed. During the relaxation the inert atoms retain their initial displacement while the active atoms are shifted until a minimum energy configuration is found. The relaxations were terminated when the force on every atom was smaller than $5.10^{-3}$ eV/Å. In this kinematical approach the simulations are done effectively at 0 K.

### 2.1.1 Dissociation into partial dislocations

The screw orientation of the superdislocation is the most interesting since it gives rise to possible dissociations and core spreading. Only two-fold and three-fold dissociations are observed experimentally (see e.g. [23-28]). We examined the core starting with three groups of initial configurations. In the first case the starting, unrelaxed configuration corresponded to the undissociated $[10\bar{1}]$ dislocation. In this case, the relaxation resulted in the same non-planar configuration reported in [19] (Fig.1). This configuration (referred to here as NP) corresponds to splitting according to the reaction

$$[10\bar{1}] \rightarrow \frac{1}{6}[11\bar{2}] + SISF_{(111)} + \frac{1}{3}[20\bar{1}] + SISF_{(1\bar{1}1)} + \frac{1}{6}[1\bar{1}\bar{2}] \qquad (1)$$

with two SISFs on the intersecting $(111)$ and $(1\bar{1}1)$ planes.

Possible planar three-fold schemes are configurations corresponding to dislocation dissociation on the $(111)$ plane according to the reaction

$$[10\bar{1}] \rightarrow \frac{1}{6}[11\bar{2}] + SISF + \frac{1}{2}[10\bar{1}] + CSF + \frac{1}{6}[2\bar{1}\bar{1}] \qquad (2)$$

which was found to be metastable in [19], and the splitting

$$[10\bar{1}] \rightarrow \frac{1}{6}[11\bar{2}] + SISF + \frac{1}{6}[2\bar{1}\bar{1}] + APB + \frac{1}{2}[10\bar{1}] \qquad (3)$$

In the case where splitting according to the reaction (2) was used as the initial configuration, the dislocation core retains the same structure. The resulting relaxed core structures are shown in Fig. 2. This configuration contains a narrow ribbon of CSF on the right-hand side (only about 2-3 lattice spacings wide) and a much wider ribbon of the SISF on the left-hand side [19]. The molecular statics technique does not guarantee that the absolute minimum of the energy is found. Several initial positions of the centre of the elastic field of the dislocation in the atomic block should therefore be tried since different starting configurations may lead to different metastable core configurations. The

locations of the initial elastic centres of the elastic fields of the dislocations were systematically varied in an attempt to identify different metastable core configurations. By varying the initial placements of the elastic centres according to reaction (2), we found a more detailed picture of the core structures obtainable for the screw superdislocation. In addition to the metastable planar core configurations reported in [19] we found a second planar core, corresponding to the same splitting of three partials with SISF and CSF on $(111)$ planes according to (2) (Fig. 2b), the energy of which is lower than the energy of first configuration. The resulting relaxed core structures, referred to here as $P_1$ and $P_2$, are almost identical (Fig. 2a and Fig. 2b). The only visible difference is that the width of the SISF of $P_2$ is about one lattice spacing $a$ (4.005 Å) wider than $P_1$. However, as we shall see later, despite the similarity between core configurations $P_1$ and $P_2$ their reaction to applied external shear stress differs.

The planar splitting according to reaction (3) was found in [7]. In these atomistic simulations the atomic interactions were described by Finnis-Sinclair type empirical central-force potentials. In what follows, we will refer to a structure as unstable that we employ as a starting configuration which relaxes into another structure, possibly a metastable one**.** It was first found in [19] that the dissociation according to reaction (3) is unstable and transforms into a configuration corresponding to reaction (2), presumably due to the appreciably lower CSF energy compared to that of the APB predicted by BOP (APB energy predicted by the Finnis-Sinclair potential is almost equal to the CSF energy [7, 15]). The variation of the initial location of the elastic centres of the splitting according to reaction (3), carried out in the present calculations, confirmed this result. Depending on the initial positions of the centres of the elastic fields of the partial dislocations, the dissociation according to reaction (3) transformed into core configurations corresponding to either $P_1$ or $P_2$.

In experiment, dissociation is often found to be two-fold in nature. We examined the core structure of the screw $[10\bar{1}]$ superdislocation starting with several initial twofold splittings, which are usually reported. If the energy of the CSF is so high that further splitting into Shockley partials is not favored then in place of reactions (2) and (3) one might expect

$$[10\bar{1}] \rightarrow \frac{1}{6}[11\bar{2}] + SISF + \frac{1}{6}[5\bar{1}\bar{4}] \qquad (4)$$

Such a configuration was observed in Al-rich TiAl [23] and in nearly stoichiometric TiAl alloys [24]. However, this dissociation was found to be unstable in the present calculations. When the splitting (4) was used as the initial configuration, the dislocation core transformed into the non-planar configuration NP (1). The subdissociation of the $\frac{1}{6}[5\bar{1}\bar{4}]$ partial and the preference for configuration (1) with SISF on the $(1\bar{1}1)$ plane to dissociation (2), is presumably due to its large Burgers vector and the much lower energy of SISF (0.140 J/m$^2$) than that of CSF (0.412 J/m$^2$) [15]. The TEM resolution, within which no evidence for subdissociation of the $\frac{1}{6}[5\bar{1}\bar{4}]$ partial was found, is about 1.5 nm [25]. It was suggested in [19] that the CSF ribbon in (2), which is only two to three lattice

spacings (about 1 nm) wide, cannot be resolved in TEM weak-beam images. The results of the atomistic simulations using BOP indicate that the planar core structures $P_1$ and $P_2$, which are found to be metastable, could be interpreted in the experimental studies as dissociation into two partials according to the reaction (4). The latter two-fold splitting is unstable, according to the present atomistic simulations, and transforms to the non-planar core NP.

Dissociation taking place according to

$$\left[10\bar{1}\right] \rightarrow \frac{1}{2}\left[10\bar{1}\right] + APB + \frac{1}{2}\left[10\bar{1}\right] \tag{5}$$

has also been reported [22, 26, 27]. It is mostly encountered after deformation above a temperature of about 300-400˚C and may largely depend on alloy composition. The results of the present atomistic simulations reveal that the dissociation (5) is also unstable. The dislocation core transformed into the planar configuration (2), corresponding to the splitting of three partials with SISF and CSF on $(111)$ planes. It was reported [25] that within the twofold dissociation according to reactions (4) and (5), the superdislocations generated at low temperatures tend in most cases to adopt the mode corresponding to the splitting (4). We believe that this result is consistent with the present atomistic simulations, showing instability of dissociation (5) and transformation to planar core (2), because of the possible interpretation due to low imaging resolution of the three-fold composition (2) as dissociation into two partials according to the reaction (4).

**We also examined the four-fold splitting into Shockley type partials on the (111) plane which involves all three stacking-fault like defects, APB, SISF and CSF according to the reaction [35]**

$$\left[10\bar{1}\right] \rightarrow \frac{1}{6}\left[11\bar{2}\right] + SISF + \frac{1}{6}\left[2\bar{1}\,\bar{1}\right] + APB + \frac{1}{6}\left[11\bar{2}\right] + CSF + \frac{1}{6}\left[11\bar{2}\right]$$

**We found that the four-fold dissociation is unstable and transforms into a configuration corresponding to reaction (2), presumably due to the high energy of the APB predicted by BOP.**

### 2.1.2 Decomposition into ordinary dislocation

In addition to the dissociations described above, the $\left[10\bar{1}\right]$ superdislocation can decompose into two ordinary dislocations with no stacking-fault like defect between them [5, 24, 28], according to the reaction

$$\left[10\bar{1}\right] \rightarrow \frac{1}{2}\left[1\bar{1}0\right] + \frac{1}{2}\left[11\bar{2}\right] \tag{6}$$

Following Veyssière we use ‘‘decomposition’’ to refer to splitting without formation of a planar fault. We found that the decomposition (6) is unstable and its core structure

depends on the initial placements of the elastic centres of the ordinary $\frac{1}{2}[11\bar{2}]$ and $\frac{1}{2}[1\bar{1}0]$ dislocations. The analysis of the relaxed core, obtained at shorter distance between the elastic centres (1.5-2.5 nm), shows that in this case the $\frac{1}{2}[11\bar{2}]$ dislocation dissociates into two partials separated by SISF on the $(111)$ plane (Fig.3a) according to the reaction

$$\frac{1}{2}[11\bar{2}] \rightarrow \frac{1}{6}[11\bar{2}] + SISF_{(111)} + \frac{1}{3}[11\bar{2}] \quad (7)$$

The relaxed core structure of the mixed $\frac{1}{2}[1\bar{1}0]$ dislocation is non-planar spread similarly, as in the case of the screw dislocation [15, 19, 20], into two non-parallel $(111)$ and $(1\bar{1}1)$ planes. The edge components also show evidence of non-planar core spreading. The relaxed structure of the core configuration shown in (Fig. 3a) is referred to here as $C_1$. With increasing the distance between the initial elastic centres of the elastic fields of the ordinary dislocations we identified a second metastable core configuration. The relaxed structure of this core configuration (referred to here as $C_2$) is shown in Fig. 3b. Detailed analysis of the structure shown in Fig. 3b reveals that the core of the $\frac{1}{2}[11\bar{2}]$ dislocation is non-planar and corresponds to dissociation according to the reaction

$$\frac{1}{2}[11\bar{2}] \rightarrow \frac{1}{6}[11\bar{2}] + SISF_{(111)} + \frac{1}{6}[13\bar{2}] + SISF_{(1\bar{1}1)} + \frac{1}{6}[1\bar{1}\bar{2}] \quad (8)$$

The relaxed core structure of the mixed $\frac{1}{2}[1\bar{1}0]$ dislocation is also non-planar. The present result suggests, that the mixed $\frac{1}{2}[11\bar{2}]$ (30° orientation) and $\frac{1}{2}[1\bar{1}0]$ (60° orientation) dislocations, which are products of the decomposition of screw superdislocations, are sessile and hardly contribute to strain when the distance between their initial elastic centres is longer than 2.5 nm.

The results of our computer simulations exhibit a clear preference of the $[10\bar{1}]$ screw superdislocation for splitting, since for all starting configurations we obtained relaxed structures corresponding to dissociation into partial dislocations. We therefore distinguish several different core structures of the screw superdislocation, depending on starting unrelaxed configurations:

1. When using either the undissociated or reaction (4) as starting configuration, the resulting core structure is the NP, reaction (1).

2. The non-planar core configuration ($C_2$) was obtained in the case of decomposition of the screw superdislocation into two mixed ordinary dislocations according to reaction (6). Such non-planar core structures are sessile and can act as strong obstacles to dislocation motion. The core $C_1$, found for the same splitting (6), corresponds to two-fold dissociation of the $\frac{1}{2}\langle 112]$ dislocation, by-product of the decomposition (6).
3. For other starting configurations, namely the planar splitting with partial dislocations according to reactions (2), (3) and (5), the relaxation resulted in a two energetically close metastable planar core configurations ($P_1$ and $P_2$) involving partial dislocations separated by SISF and CSF. Since BOP for γ TiAl, in agreement with ab-initio calculations, predicts the energy of CSF (0.412 J/m$^2$) to be lower than that of APB (0.545 J/m$^2$) [15, 16], the preference for configuration (2) is to be expected

**2.2 Effects of applied stress**

**2.2.1 Dissociated cores $P_1$ and $P_2$**

In order to study the glide of the planar core configurations under the effect of externally applied shear stress we started with simulation blocks containing the fully relaxed core structures $P_1$ and $P_2$ of a $[10\bar{1}]$ screw superdislocation. The shear stress was applied in the $[10\bar{1}]$ direction in such a way that the dislocations were set to glide on a $(111)$ plane. In practice, this stress is imposed by applying the appropriate homogeneous shear strain, which is evaluated with anisotropic elasticity theory. The shear strain was gradually increased in small increments and the block fully relaxed after each step.

Under the effect of externally applied shear stress such that the $\frac{1}{6}[11\bar{2}]$ partial would be leading during glide, the dislocation configuration $P_1$ transformed into the non-planar form (1) at a stress of $0.002C_{44}$. An identical result was reported in [19]. In contrast, despite the similarity between configurations $P_1$ and $P_2$, when applying the same shear stress on the planar core $P_2$ the dislocation starts to move on the $(111)$ plane at a stress of $0.005C_{44}$. After gliding a distance of about 3 nm, the core configuration $P_2$ transforms into the non-planar form (1) at a stress of $0.026C_{44}$ (Fig. 4). The dislocation thus became completely locked similar to the core structure $P_1$. Both planar core configurations react similarly when the shear stress is applied such that the $\frac{1}{6}[11\bar{2}]$ partial would be trailing during glide. After starting to move on $(111)$ at a stress of $0.01C_{44}$, the dislocation core structures transformed into that shown in Fig. 5a after increasing the applied stress to $0.045C_{44}$. This configuration is planar, though with the CSF, bounded by $\frac{1}{6}[1\bar{2}1]$ and $\frac{1}{6}[2\bar{1}\,\bar{1}]$ partials, one layer above that of the unstressed state. By increasing the externally applied shear stress, the entire core configuration (2) moves one layer above that of the initial position. A dipole of twinning partials $\frac{1}{6}[11\bar{2}] + SISF + \frac{1}{6}[\bar{1}\,\bar{1}\,2]$ remains in the initial $(111)$ layer (Fig. 5b). The applied stress contracts the dipole until

finally the twinning partials annihilate leaving the core configuration (2) one layer above that of its initial position.

### 2.2.2 Decomposed cores $C_1$ and $C_2$

We also studied the response of the core configurations $C_1$ and $C_2$ to externally applied shear stress. The stress was applied in such a way that the dislocations were set to glide on the $(111)$ plane. If the stress in this plane acts such that the $\frac{1}{2}[11\bar{2}]$ dislocation of reaction (6) would be leading, both ordinary dislocations retain their non-planar core structure in the case of core configuration $C_2$. The core structure $C_1$ transforms into the non-planar form (1) at a stress of $0.05C_{44}$. Both core configurations $C_1$ and $C_2$ thus became completely locked in this case.

A different situation arises when the shear stress in the $(111)$ plane is applied such that the $\frac{1}{2}[11\bar{2}]$ dislocation of reaction (6) would be trailing. At a stress of $0.034C_{44}$, the core structure $C_1$ transforms into planar configuration (2), corresponding to splitting into three partials with SISF and CSF on the $(111)$ plane (Fig. 2). In the case of configuration $C_2$, the applied stress extends the core structure of the $\frac{1}{2}[1\bar{1}0]$ ordinary dislocation one layer above that of the unstressed state and contracts the SISF on the $(111)$ plane (Fig. 6a). When the $\frac{1}{6}[11\bar{2}]$ partial bounding the SISF reaches the $\frac{1}{6}[13\bar{2}]$ dislocation, the initial splitting of the $\frac{1}{2}[11\bar{2}]$ dislocation transforms into

$$\frac{1}{2}[11\bar{2}] \rightarrow \frac{1}{6}[1\bar{1}\bar{2}] + SISF_{(1\bar{1}1)} + \frac{1}{3}[010] + SISF_{(111)} + \frac{1}{3}[11\bar{2}] \qquad (9)$$

This transformation is accompanied by dissociation of the ordinary $\frac{1}{2}[1\bar{1}0]$ dislocation to CSF bounded by two partials on the adjacent plane (Fig. 6b)

$$\frac{1}{2}[1\bar{1}0] \rightarrow \frac{1}{6}[1\bar{2}1] + CSF_{(111)} + \frac{1}{6}[2\bar{1}\bar{1}] \qquad (10)$$

With increasing applied shear stress, a $[10\bar{1}]$ superdislocation composed of three partials with SISF and CSF according to the reaction (2) is formed one layer above the initial $(111)$ plane (Fig. 6c). A non-planar sessile combination containing two SISFs, with $\frac{1}{6}[1\bar{1}\bar{2}]$, $\frac{1}{3}[010]$ and $\frac{1}{6}[\bar{1}\bar{1}2]$ partial dislocation bounding the faults, remains in the $(111)$ and $(1\bar{1}1)$ planes.

In the next section we discuss some implications of the dissociated configurations and their response to externally applied shear stress obtained in the present atomistic study on dislocation dynamics, including the mechanism of locking and the issue of dislocation decomposition.

## 3. DISCUSSION

The mobility of $\langle 101]$ superdislocations is naturally closely related to their core structure**. Experimental observations in the low temperature regime show that screw dislocations dominate during in situ deformation. Screw segments are of most interest since they may cross slip. The cores of dissociated screw superdislocations may either extend on their slip plane, resulting in a glissile configuration, or cross slip on the conjugate** $(1\,\bar{1}\,1)$ **leading to low mobility.** The planar splitting of the screw $\langle 101]$ superdislocation, involving both the SISF and CSF, is glissile with significantly lower Peierls stress than that of ordinary dislocations [19, 20]. The existence of glissile and sessile dislocation dissociations of the $\langle 101]$ superdislocation have important implications for the deformation behaviour of $L1_0$ TiAl. Since ordinary $\frac{1}{2}\langle 110]$ dislocations have sessile non-planar cores, the glide of these dislocations becomes significant only at high temperatures. The precision of atomistic simulations is not sufficient to decide which of the metastable configurations is energetically favored. **Using the anisotropic elastic theory of singular dislocations we could attain a better physical understanding of the outcomes of atomistic simulations. The energy of the planar configurations of the suprdislocation dissociated into three partials separated by stacking fault type defects can be written as [15, 22]**

$$E(x,y)=\sum_{i=1}^{3}K_i^{self}\ln\frac{R}{r_0}+K_{12}\ln\frac{R}{x}+K_{23}\ln\frac{R}{y}+K_{13}\ln\frac{R}{x+y}+\gamma_{SISF}(x-r_0)+\gamma_{CSF}(y-r_0) \quad \textbf{(11)}$$

**Where $K_{ij}$ are energy factors for interaction and $K_i^{self}$ is the energy factor for self interaction of the partial *i*, *x, y* are the separations between the partials, γ is the energy of the stacking-fault type defect connecting the two partials, R is the outer cut-off radius and $r_0$ the inner cut-off radius, often associated with the width of the dislocation core. The energy in the above expression depends on two parameters - the widths of the CSF and SISF and is obviously determined only up to an additive constant.**

**The equilibrium splitting distances $x_0$ and $y_0$ are determined by minimizing *E(x,y)* with respect to both x and y. The energy of the sessile non-planar splitting according to (1) has similar form. The equilibrium width of splitting is again determined by minimization of the energy with respect to the separations between the partials. The anisotropic elasticity analysis does not allow us to compare directly**

**the energies of the competing metastable configurations since the energies can be determined only up to an additive constant [15, 22]. Using the energies of SISF and CSF determined in the framework of the BOP for TiAl, the widths of the SISF and CSF are correspondingly 38.47 Å and 11.14 Å [15]. The widths of the stacking faults corresponding to planar core structures $P_1$ and $P_2$ determined by the present atomistic simulations are close to these values; x~37 Å, y~12 Å for core $P_1$ and x~39 Å, y~12 Å for $P_2$.**

**The existence of two different planar core structures $P_1$ and $P_2$, predicted by the atomistic simulations, cannot be explained from the standpoint of linear elasticity theory. In order to understand the reason for the differences between the predictions of the anisotropic elastic theory and atomistic simulations, we have to take into account that (11) does not include the effect of the crystal lattice, which can be represented by a periodic energy function of the dislocation position [22]. The periodic energy variations reflect the changes in dislocation core energy as dislocation translates from one lattice position to the next. Such periodic energy variation cannot be explained from the standpoint of linear elasticity theory. The continuum theory breaks down near the dislocation centre, where lattice discreteness and non-linearity of interatomic interactions become important. The analyses of the results of the atomistic simulations and comparison with the widths of SISF and CSF calculated by using anisotropic elastic theory indicate that the positions of the partial dislocations are at the corresponding Peierls valleys in the case of core $P_2$. It can be concluded, that the partial dislocations are not situated at the preferred positions, marked by the minima of the energy functions in the case of core configuration $P_1$. In this case the lattice resistance compensates the increased repulsive force between $\frac{1}{6}[11\bar{2}]$ and $\frac{1}{2}[10\bar{1}]$ dislocations due to the smaller width of SISF.**

**The cross-slip of the planar configuration of superdislocation on conjugate $(1\bar{1}1)$ plane occurs in response to applied external and internal stress.** Yoo [30] proposed that in an elastically anisotropic material such as TiAl, the forces between the partial dislocations produce a torque that pushes the planar core of dislocation off the octahedral glide plane. Yoo and Fu [31] have calculated the anisotropic interaction forces on dissociated screw dislocations in γ-TiAl. The Yoo torque promotes the formation of sessile core configuration through cross-slip of CSF, forming SISF located on the $(1\bar{1}1)$ plane. **An applied external shear stress σ generates a Peach-Koehler force on the partial dislocations and produces effective fault energies $\Gamma = \gamma + \frac{1}{2}(F_1 - F_2)$ in the expression for the energy (11), where $F_1$ and $F_2$ are the glide components of the forces acting on the partial dislocations bounding the faults [22, 34]. One sees that the width of the fault increases if $F_1 - F_2 < 0$ and decreases if $F_1 - F_2 > 0$. In order to estimate the driving force for cross-slip on $(1\bar{1}1)$ plane using the anisotropic elastic theory, the cross-slipped segment can be assumed to occur after constriction of the CSF on one portion of the dislocation line [34]. Once the $\frac{1}{6}[2\bar{1}\bar{1}]$ partial dislocation**

**is constricted, the driving force can be estimated by varying the length of the cross-slipped segment and calculating the energy of the non planar dislocation core [34].**

The atomistic simulations show that the ability of the superdislocation in its planar core configurations to glide depends strongly on the sense of shearing [19]. The glide of metastable core configurations $P_1$ and $P_2$, corresponding to the planar splitting, was found to be very different depending on whether the $\frac{1}{6}[11\bar{2}]$ partial bounding the SISF is leading or trailing. In the latter case they remain glissile, while in the former case the glissile planar core transforms into a sessile one. Application of shear stress corresponding to different orientations of the maximum resolved shear stress with respect to the $(111)$ plane, indicates that the transformation of the planar core configurations into the non-planar form is principally controlled by the shear stress in the cross-slip plane $(1\bar{1}1)$. If the stress in the $(111)$ plane acts such that the $\frac{1}{6}[11\bar{2}]$ partial of the splitting would be leading during glide, the resolved shear stress (RSS) on the cross-slip plane $(1\bar{1}1)$ plane acts to drive the $\frac{1}{6}[1\bar{1}\bar{2}]$ partial dislocation (Fig. 4) in a direction extending the SISF in this plane. The sessile structure forms in this case since both RSS and the Yoo torque assist creation of the correct stacking fault on the cross-slip plane [19, 32].

The opposite situation arises when the shear stress in the $(111)$ plane is applied such that the $\frac{1}{6}[11\bar{2}]$ partial of $P_1$ and $P_2$ would be trailing. In this case, the RSS on the secondary octahedral plane promotes the formation of a high-energy non-planar configuration with a CSF. Since the elastic anisotropy interaction force does not change with the orientation or applied load, the Yoo torque acts against the RSS in the opposite orientation of the applied shear stress and mitigates the importance of the secondary RSS. The combined action of the RSS on the cross-slip $\{111\}$ planes together with the Yoo torque does not lead to the formation of a stacking fault on the cross-slip plane. Instead, the applied external stress promotes the formation of a new planar configuration with the CSF on an adjacent $(111)$ layer, followed by the reproduction of the core configurations $P_1$ and $P_2$ on a layer above that of their initial location (Fig. 5).

In spite of the differences in the glide of core configurations $P_1$ and $P_2$ in such direction that the $\frac{1}{6}[11\bar{2}]$ partial would be leading, they both tend to transform into a non-planar core structure. This mechanism occurs immediately when the stress is applied on the core $P_1$, while the transformation of $P_2$ into a sessile core occurs only at higher applied stress and after some limited glide. **The differences in the transformation of planar configurations $P_1$ and $P_2$ into a non-planar core structure when the $\frac{1}{6}[11\bar{2}]$ partial would be leading during glide also cannot be explained from the stand point of linear elasticity theory. The existence of two planar core structures $P_1$ and $P_2$ and their different responses to applied external stress result from changes in partial dislocation core energy as an effect of lattice discreteness and non-linearity of interatomic interactions near the dislocation centre.** Presumably, in the case of core

configuration $P_2$ the partials are blocked in deeper Peierls valleys than in $P_1$. **Hence, the possible splitting into the $(1\bar{1}1)$ cross-slip plane extends at higher RSS, necessary for overcoming the energy barrier for formation of the sessile core configuration.**

The results of the atomistic simulations, showing that in the screw orientation $\langle 101]$ dislocations possess glissile metastable core structures, indicate that superdislocation activity can be expected at lower temperatures. This is, indeed, observed in single phase TiAl where several experimental studies identified superdislocation slip as the major deformation mode at lower temperatures (see e.g. [4, 24]). As the temperature increases, all dislocations become relatively mobile, but the superdislocations become increasingly blocked as they adopt a thermally activated non-planar configuration [24]**. At high temperatures the superdislocations show a shape typical of locking-unlocking mechanisms.** The explanation of thermally activated effects is beyond of the applicability of the present molecular statics simulations, but our core structures are likely candidates for these observed non-planar configurations.

In addition to the dominant $\langle 101]\{111\}$ slip system, experimental studies [24, 25, 27] encounter situations in single crystal γ-TiAl deformed at low temperatures, involving $\frac{1}{2}\langle 112]$ and $\frac{1}{2}\langle 110]$ dislocations, themselves glissile in the same $\{111\}$ plane as the superdislocations. It is argued [25] that the only sources to operate are of superdislocations, $\frac{1}{2}\langle 110]$ dislocations are moderately mobile and $\frac{1}{2}\langle 112]$ dislocations are the least mobile of all. The latter are left in the crystal wherever decomposition of superdislocations according to reaction (6) takes place. We found two metastable core structures corresponding to the two-fold decomposition into ordinary $\frac{1}{2}[11\bar{2}]$ and $\frac{1}{2}[1\bar{1}0]$ dislocations. The present atomistic study reveals that the relaxed core structure of the mixed $\frac{1}{2}[1\bar{1}0]$ dislocation, which is a by-product of the decomposition (6), is non-planar. We have observed no dissociation of the $\frac{1}{2}[1\bar{1}0]$ dislocation into Shockley partials separated by stacking fault type defect. The reason is, apparently, the high energy of the CSF in $L1_0$ TiAl. It was suggested [25] that $\frac{1}{2}\langle 112]$ dislocations could dissociate further to SISF bounding two-fold dissociation according to reaction (7), that in its turn may spontaneously transform into the configuration containing SISF and superlattice extrinsic stacking fault (SESF) [7]. Though the two-fold dissociation (7) was found in the present atomistic simulations (core configuration $C_1$), we have not obtained a core structure containing SESF. The configuration with SESF formed within the core was observed in atomistic simulations of the core of a $\frac{1}{2}\langle 112]$ screw dislocation [29]. Alternatively, the present atomistic simulations predict that at longer distance between the elastic centres of the ordinary dislocations, the mixed $\frac{1}{2}\langle 112]$ dislocations dissociate into three partials

bounding two SISFs on the intersecting $(111)$ and $(1\bar{1}1)$ planes (reaction (8), Fig. 3b). In this case, the $\frac{1}{2}\langle 112]$ and $\frac{1}{2}\langle 110]$ dislocations, which are products of the decomposition of the screw superdislocation, are sessile and hardly contribute to strain. The analysis of the core structure $C_2$ under stress suggests that ordinary $\frac{1}{2}\langle 110]$ dislocations are relatively more mobile than the $\frac{1}{2}\langle 112]$ dislocations dissociated into two SISFs on the intersecting $(111)$ and $(1\bar{1}1)$ planes.

Following the results of the present atomistic simulation we may speculate on a mechanism for formation of ordinary $\frac{1}{2}\langle 110]$ dislocations from the decomposition of $\langle 101]$ screw superdislocations. We found that the core structure corresponding to reaction (6) depends on the initial placements of the elastic centres of the ordinary $\frac{1}{2}[11\bar{2}]$ and $\frac{1}{2}[1\bar{1}0]$ dislocations. When the distance between the elastic centres is less than 1.5 nm the decomposition according to reaction (6) is unstable and transforms into a planar splitting into three partials with SISF and CSF on $(111)$ plane corresponding to reaction (2) (Fig.2). We observe formation of a $\frac{1}{2}[1\bar{1}0]$ dislocation with increasing distance between the elastic centres. At slightly longer distance between the elastic centres (1.5-2.5 nm) the splitting (6) transforms into core $C_1$ with the $\frac{1}{2}[11\bar{2}]$ dislocation dissociated into two partials separated by SISF according to reaction (7) (Fig. 3a). The results of the atomistic simulations indicate that the planar core (2) may transform into the $C_1$ providing a mechanism for the generation of ordinary $\frac{1}{2}[1\bar{1}0]$ dislocations. This could originate from the decomposition of the $\frac{1}{2}[10\bar{1}]$ partial from planar splitting (2) according to reaction

$$\frac{1}{2}[10\bar{1}] \rightarrow \frac{1}{3}[11\bar{2}] + \frac{1}{6}[1\bar{2}1] \qquad (11)$$

(see Fig. 2c). This decomposition is followed by the transformation of the two partials $\frac{1}{6}[1\bar{2}1]$ and $\frac{1}{6}[2\bar{1}\bar{1}]$ separated by CSF into an ordinary $\frac{1}{2}[1\bar{1}0]$ dislocation due to the high energy of the CSF in $L1_0$ TiAl. The remaining configuration corresponds to core structure $C_1$.

The present atomistic simulations indicate that the ability of the superdislocation to glide in its two-fold splitting into ordinary $\frac{1}{2}\langle 112]$ and $\frac{1}{2}\langle 110]$ dislocations also depends strongly on the sense of shearing. The transformations of both metastable core configurations $C_1$ and $C_2$ were found to be very different depending on whether the $\frac{1}{2}\langle 112]$ dislocation of reaction (6) is leading or trailing. In the latter case they both transform into configurations containing the planar composition of three partials with SISF and CSF on the $(111)$ plane (2) within the core. When external shear stress was applied on the core $C_2$ we observed formation of CSF on an adjacent $(111)$ layer, followed by the development of the planar combination of partials (2) on the adjacent $(111)$ plane. The shear-induced extension of the CSF is due to splitting of the ordinary $\frac{1}{2}[1\bar{1}0]$ dislocation into two partials, initiated by interaction with the dissociated $\frac{1}{2}\langle 112]$ dislocation. The formation of planar core configuration (2) on the adjacent $(111)$ plane is identical to the one we obtained while studying the glide of the planar core structures $P_1$, $P_2$ and $C_1$ (Fig. 5b). However, in the case of core structure $C_2$, the remaining configuration of three partials with SISF in the initial $(111)$ plane and second SISF in the cross-slip $(1\bar{1}1)$ is non-planar (Fig. 6c). This sessile structure anchors the planar core configuration (2) lying on the adjacent $(111)$ plane. In the case of core $C_1$, the transformed configuration is identical to the planar structure (2) and therefore more glissile that core $C_2$.

Under the effect of externally applied stress such that the ordinary $\frac{1}{2}[11\bar{2}]$ dislocation of reaction (6) would be leading the core configurations $C_1$ and $C_2$ transform into sessile structures. The sessile screw segments of superdislocations will act as obstacles for dislocation motion and thus it can be expected that the yield stress will be higher when the $\frac{1}{6}[11\bar{2}]$ partials bounding the SISF or $\frac{1}{2}[11\bar{2}]$ of reaction (6) are leading. This has indeed been observed [4, 33].

**The metastable stacking-fault-type defects on the $(111)$ planes are therefore very important as they determine possible dislocation splittings and their energies control the extent of these dissociations. Central force schemes are not predictive as far as the energies of the planar faults are concerned. The most likely reason is that these potentials exclude any covalent type bonding [17]. Therefore, cores of $[10\bar{1}]$ superdislocation predicted by central force schemes [7] are in this case not those found either in experiment or in our simulations. Importantly, owing to the fact that directional bonding is included in the BOP scheme, the potential captures the fault energies accurately. The agreement between BOP and ab-initio calculations is very satisfactory [16].**

## CONCLUSIONS

Atomistic simulations of the core structure and glide of the screw $\langle 101]$ superdislocation have been made using a bond order potential for γ-TiAl. We examined the core structure of the screw $\langle 101]$ superdislocation starting with initial unrelaxed configurations corresponding to various dislocation dissociations, discussed in the literature. In the screw orientation the superdislocations were found to possess planar and non-planar metastable core structures. The possible splitting into partials bounding high-energy APB, as well as dissociation to dislocations with large Burgers vectors, $\frac{1}{6}\langle 514]$ and $\frac{1}{2}\langle 112]$, were found to be unstable. The analysis of the core structures indicate that superdislocation activity can be expected to dominate at lower temperatures. The results of the present atomistic simulations suggest that at low temperatures the ordinary $\frac{1}{2}\langle 112]$ and $\frac{1}{2}\langle 110]$ dislocations, which are sessile and hardly contribute to strain, are products of the decomposition of superdislocations.

We studied the response of our core configurations to externally applied shear stress. The effect of applied shear stress on the glide and core structure of the superdislocation, at stresses much higher that the stress at which the dislocation starts to move, can be assessed only by large cells and long-time atomistic simulations. The parallel version of the OXON-Penn-BOP code is essential for making such simulations. In violation of Schmid's law, the transformations of the core structures and the ability of the dislocation in its planar core configurations to glide depend strongly on the sense of shearing. The planar cores transform into a non-planar core structure under the effect of externally applied shear stress such that the $\frac{1}{6}[11\bar{2}]$ partial bounding the SISF would be leading during glide. When stress is applied in reverse direction ($\frac{1}{6}[11\bar{2}]$ partial would be trailing) the entire glissile core configuration gradually moves on an adjacent $(111)$ layer. This process is accompanied by formation of a dipole of twinning partials on the initial $(111)$ plane, which annihilates with increasing stress. Similar composition of three partials with SISF and CSF according to reaction (2) is formed when shear stress is applied on the core configurations $C_1$ and $C_2$, such that the $\frac{1}{2}\langle 110]$ dislocation of reaction (6) would be leading during glide. However, in the case of core structure $C_2$, the planar composition (2) is expected to be less mobile, since it is anchored by a non-planar configuration of three partials with SISF in the initial $(111)$ plane and second SISF in the cross-slip $(1\bar{1}1)$ plane. The simulated response of the dissociated configurations $P_1$, $P_2$, $C_1$ and $C_2$ to externally applied shear stress is consistent with the observed tension-compression asymmetry of the yield stress in $L1_0$-TiAl.

**ACKNOWLEDGEMENTS** The authors wish to thank Prof. V. Vitek of the University of Pennsylvania for helpful discussions during the course of this work. This research was supported by the EPSRC, under grant no. EP/E025854/1 and by a grant from HPC-Europa.



**REFERENCES**

[1] Kim, Y.-W., 1989, Intermetallic alloys based on gamma titanium aluminide. JOM 41, 24.

[2] Appel, F., Wagner, R., Mater. Sci. Eng. R22, 1998, 187.

[3] Yamaguchi M., Inui, H., Yokoshima S., Kishida K. and Johnson D. R., Mat. Sci. Eng. A 213, 1996, 25.

[4] Inui, H., Matsumuro, M., Wu, D.-H., and Yamaguchi, M., Phil. Mag. A 75, 1997, 395.

[5] Hug G., Loiseau A. and Veyssière P., Phil. Mag. A 57, 1988, 499.

[6] Girshick A. and Vitek V., High-Temperature Ordered Intermetallic Alloys VI, edited by J. Horton, I. Baker, S. Hanada, R. D. Noebe and D. Schwartz (Pittsburgh, Materials Research Society), 364, 1995, 145.

[7] Mahapatra R., Girshick A., Pope D.P. and Vitek V., Scripta Metall., 33, No. 12, 1995, 1921.

[8] Panova J. and Farkas D., Philos. Mag. A 78, 1998, 389.

[9] Simmons J. P., Rao S. I. and Dimiduk D. M., Philos. Mag. A **75**, 1997, 1299.

[10] Woodward C. and Rao S. I., Phil. Mag. A 84, 2004, 401.

[11] Pettifor, D. G., Phys. Rev. Lett. 63, 1989, 2480.

[12] Aoki, M. and Pettifor, D. G., in "Physics of Transition Metals," eds. P. M. Oppeneer and J. Kubler (World Scientific, Singapore, 1993, 299.

[13] A J Skinner A. J. and Pettifor D. G., J. Phys.: Condens. Matter 3, 1991, 2029.

[14] Nguyen-Manh, D., Pettifor, D.G., Znam , S., and Vitek, V., 1998, in "Tight-Binding Approach to Computational Materials Science", edited by P.E.A. Turchi, A. Gonis and L. Colombo (Pittsburgh, Materials Research Society) Vol. 491, 1998, 353.

[15] Znam S., PhD Thesis, University of Pennsylvania, 2001.

[16] Znam S., Nguyen-Manh D., Pettifor D. G. and Vitek V., Phil. Mag A 83, 2003, 415.

[17] Vitek V., Ito K., Siegl R. and Znam S., Mat. Sci. Eng. A 240, 1997, 752.

[18] Ehmann J. and Fähnle M., Philos. Mag. A 77, 1998, 701.

[19] Porizek R., Znam S., Nguyen-Manh D., Vitek V. and Pettifor D.G., Mat. Res. Soc. Symp.Proc. vol. 753, 2003, BB4.3.1.

[20] Katzarov I. H., Cawkwell M. J., Paxton A.T. and Finnis M. W., Phil. Mag 87, 2007, 1795.

[21] Horsfield A.P., Bratkovsky A.M., Fearn M., Pettifor D.G., and Aoki M., Phys. Rev. B 53, 1996, 12694.

[22] Hirth, J. P. and Lothe, J., Theory of Dislocations, 2nd edn. Wiley-Interscience, New York, 1982.

[23] Stucke, M. A., Vasudevan, V. K., and Dimiduk, D. M., Mater. Sci. Eng. A192/193, 1995, 195.

[24] Sriram, S., Vasudevan, V. K., and Dimiduk, D. M., Mater. Sci. Eng. A192/193, 1995, 217.

[25] Gregori F. and Veyssère P., Philos. Mag. A 80, 2000, 2913.

[26] Wang, Z.-M., LI, Z.X., and Whang, S. H., Mater. Sci. Engng, A192± A193, 1995, 211.

[27] Jiao S., Bird N., Hirsch P. B., and Taylor G., Phil. Mag. A 78, 1998, 777.

[28] Hug G., Loiseau A. and Lasalmonie A., Phil. Mag. A 54, 1986, 47.

[29] Katzarov I.H., Unpublished, 2007.

[30] Zupan M., Hemker K.J., Acta Mat. 51, 2003, 6277.

[31] Yoo M. H. Acta Metall 35, 1987, 1559.

[32] Yoo M. H, Fu C. L., Metall Mater Trans A 29, 1998, 49.

[33] Inui H. and Yamaguchi M., Electron Microscopy 32, 1997, 144.

[34] Woodward C. and MacLaren, Phil. Mag., A 74, 1996, 337.

[35] Vitek V., Rerrin R. C. and Bowen D. K., Phil. Mag. A 21, 1970, 1049.

## FIGURE CAPTIONS

Fig. 1 Differential displacement map of the non-planar splitting of $[10\bar{1}]$ screw superdislocation in $(111)$ and $(1\bar{1}1)$ planes. All atomic displacements are normal to the plane of the paper; the lengths of arrows describe the amount of relative displacement of pairs of atoms [35].

Fig. 2 Differential displacement map of the planar splitting of $[10\bar{1}]$ screw superdislocation in the $(111)$ plane. (a) Core structure $P_1$. (b) Core structure $P_2$. Schematic picture shows corresponding dissociation. (c) Schematic picture showing formation of ordinary $\frac{1}{2}\langle 110]$ dislocation from the planar splitting of $[10\bar{1}]$ screw superdislocation. In this and following schematic pictures partial dislocations' cores are represented by circles with radius proportional to Burgers vectors.

Fig. 3 Differential displacement map of $[10\bar{1}]$ screw superdislocation decomposed into ordinary $\frac{1}{2}[11\bar{2}]$ and $\frac{1}{2}[1\bar{1}0]$ dislocations. (a) Core structure $C_1$. The apparent planar fault

to the right of the $\frac{1}{3}[1\,1\,\bar{2}]$ dislocation is in fact a part of spreading of its core. (b) Core structure $C_2$. Schematic pictures show corresponding dissociations.

Fig. 4 Effect of the shear stress applied in the $(111)$ plane on the planar splitting $P_2$ such that the $\frac{1}{6}[1\,1\,\bar{2}]$ partial bounding the SISF is leading.

Fig. 5 Effect of the shear stress applied in the $(111)$ plane on the planar splitting $P_2$ such that the $\frac{1}{6}[2\,\bar{1}\,\bar{1}]$ partial bounding the CSF is leading. (a) The core structure at a stress of $0.045C_{44}$. (b) The core structure at a stress of $0.06C_{44}$. Schematic pictures show corresponding dissociations. The dipole mentioned in the text is bound by SISF. The dipole at the centre of the figure is stabilized by the applied stress.

Fig. 6 Effect of the shear stress applied in the $(111)$ plane on the planar splitting $C_2$ such that the $\frac{1}{2}[1\,\bar{1}\,0]$ ordinary dislocation is leading. (a) The core structure at a stress of $0.045C_{44}$. (b) The core structure at a stress of $0.06C_{44}$. (c) The core structure at a stress of $0.065C_{44}$. Schematic pictures show corresponding dissociations.

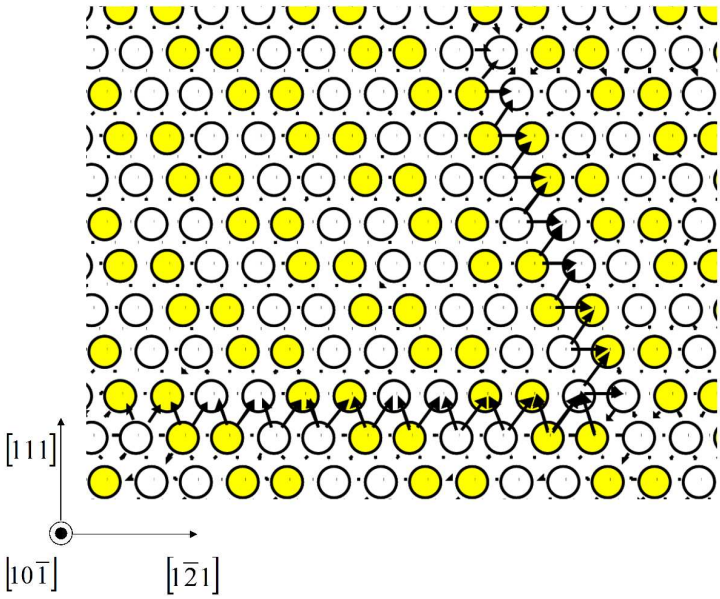


Figure 1
279x215mm (300 x 300 DPI)

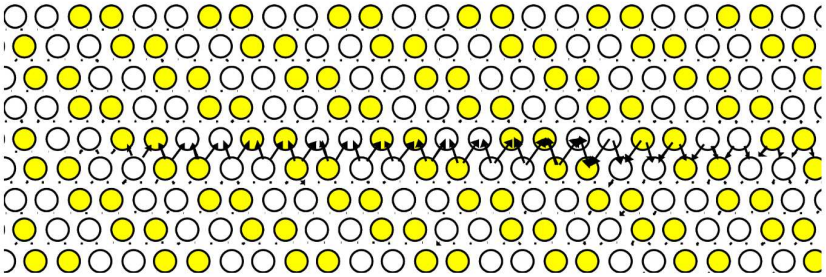

Figure 2a
279x215mm (300 x 300 DPI)

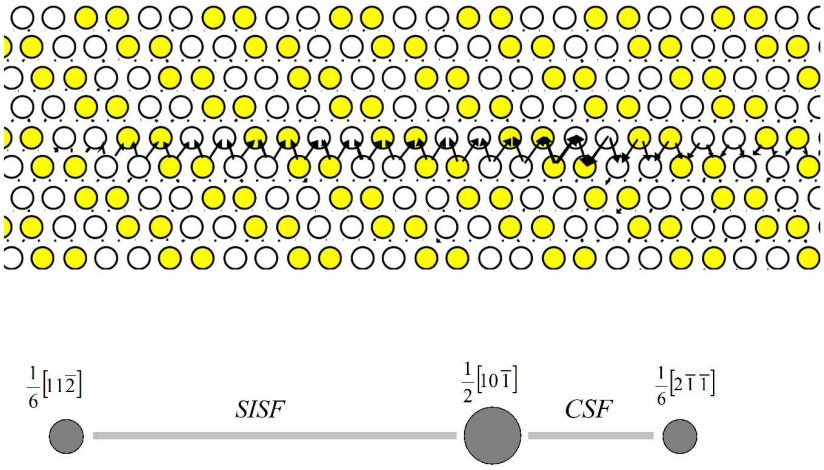


Figure 2b
279x215mm (300 x 300 DPI)

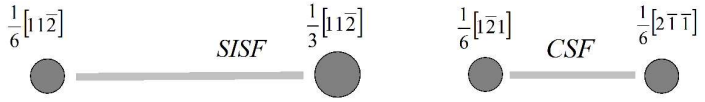


Figure 2c
279x215mm (300 x 300 DPI)

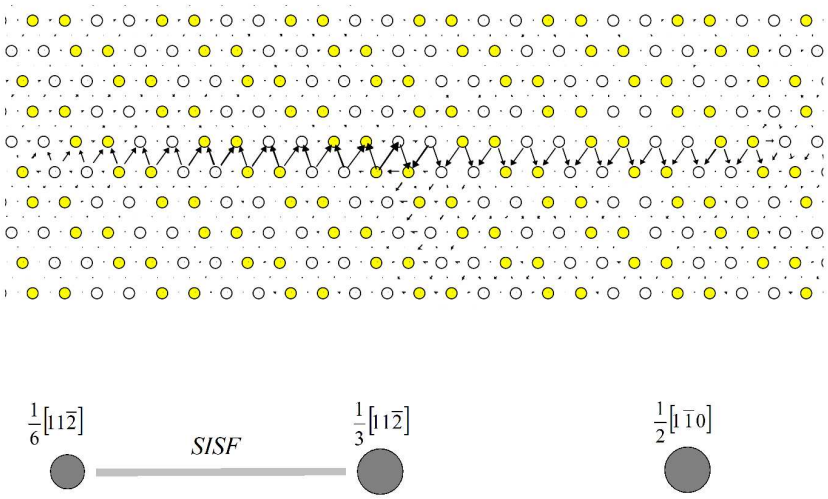


Figure 3a
279x215mm (300 x 300 DPI)

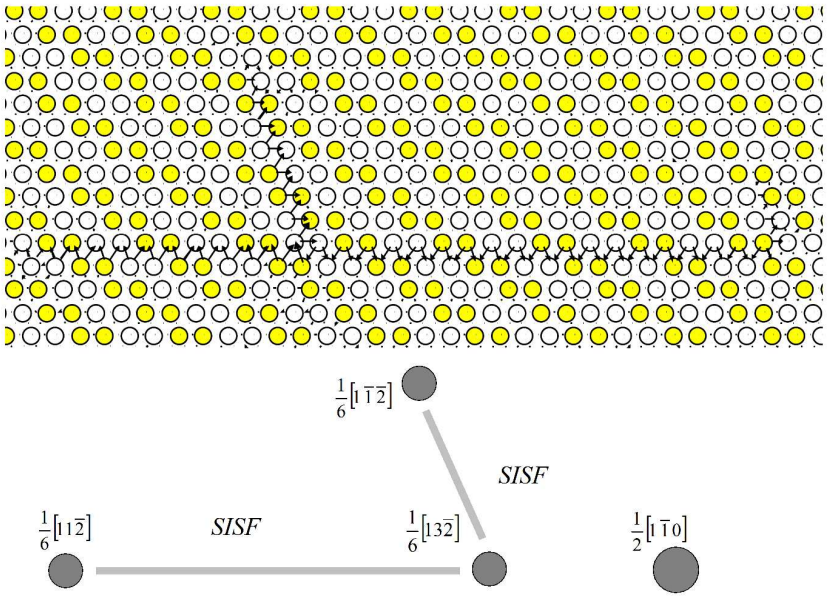


Figure 3b
279x215mm (300 x 300 DPI)

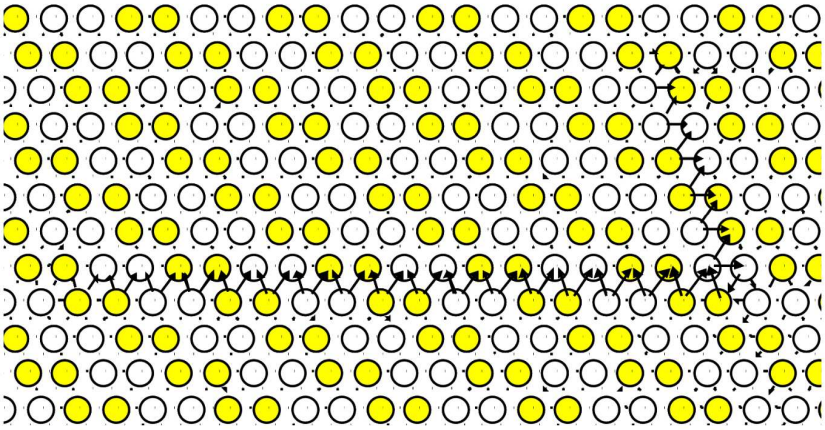

Figure 4
279x215mm (300 x 300 DPI)

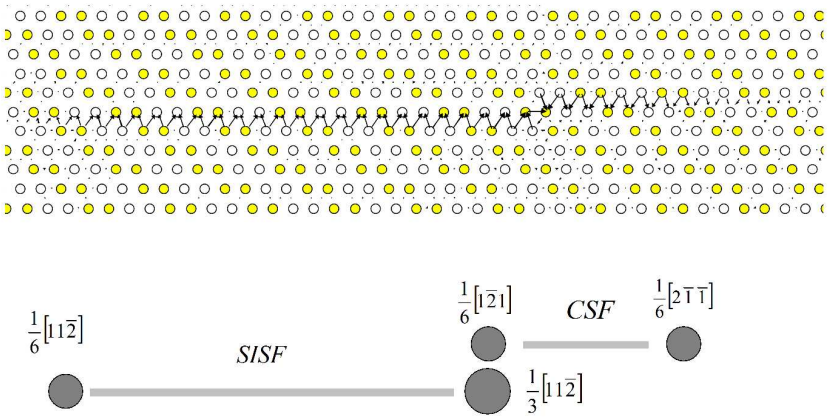


Figure 5a
279x215mm (300 x 300 DPI)

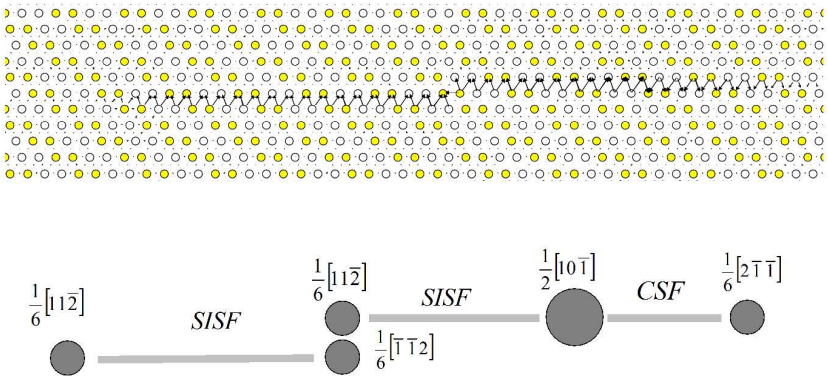


Figure 5b
279x215mm (300 x 300 DPI)

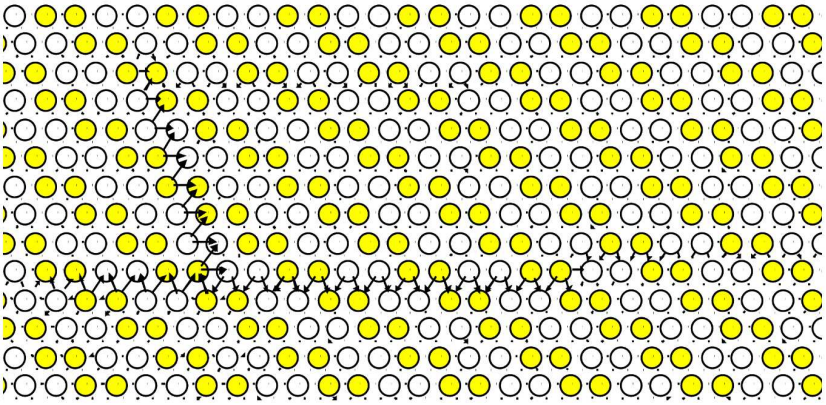

Figure 6a
279x215mm (300 x 300 DPI)

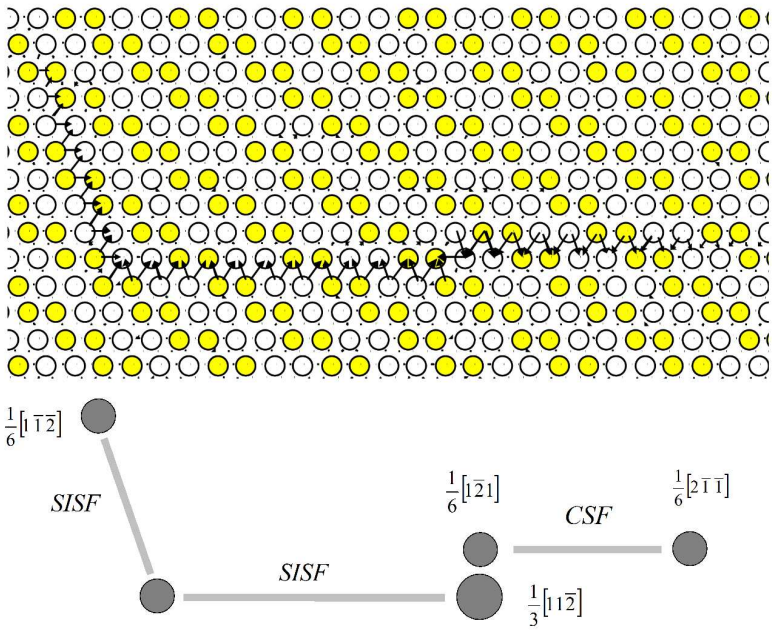


Figure 6b
279x215mm (300 x 300 DPI)

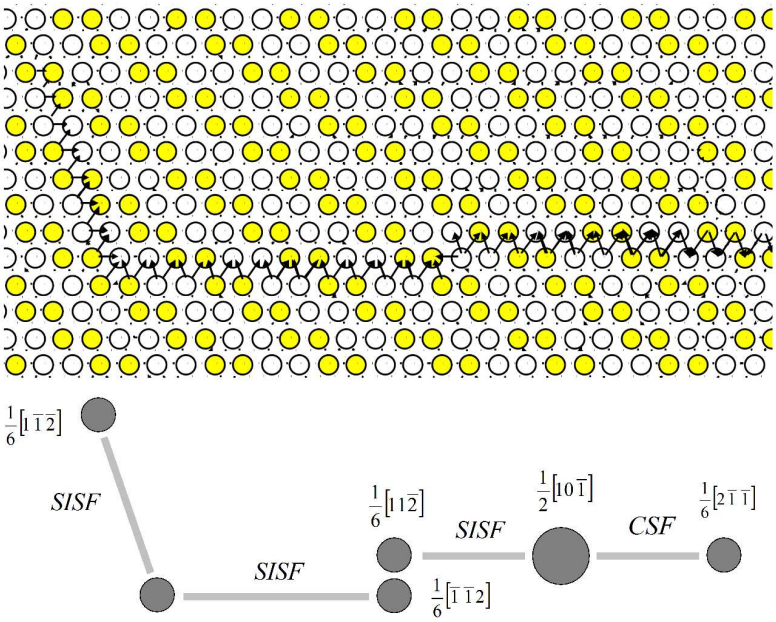


Figure 6c
279x215mm (300 x 300 DPI)